Original article

In silico studies on the anti-acne potential of *Garcinia mangostana* xanthones and benzophenones

Natalia Blicharska[1], Ziyad Ben Ahmed[2,3], Simon Jackson[4], Dino Rotondo[1], Veronique Seidel[1*]

[1] Strathclyde Institute of Pharmacy & Biomedical Sciences, University of Strathclyde, Glasgow, UK

[2] Laboratory of Fundamental Science, University Amar Telidji, Laghouat, Algeria

[3] Department of Analytical Chemistry, Applied Chemometrics and Molecular Modelling, Vrije Universiteit Brussel (VUB), Brussels, Belgium

[4] Botanical Research Department, Davines S.p.A. Via Don Angelo Calzolari 55/A, 43126 Parma, Italy

* Correspondence: Veronique Seidel (veronique.seidel@strath.ac.uk)

Abstract:

Garcinia mangostana fruits are used traditionally for inflammatory skin conditions, including acne. In this study, an *in silico* approach was employed to predict the interactions of *G. mangostana* xanthones and benzophenones with three proteins involved in the pathogenicity of acne, namely the human JNK1, *Cutibacterium acnes* KAS III and exo-β-1,4-mannosidase. Molecular docking analysis was performed using Autodock Vina. The highest docking scores and size-independent ligand efficiency values towards JNK1, *C. acnes* KAS III, and exo-β-1,4-mannosidase were obtained for garcinoxanthone T, gentisein/2,4,6,3',5'-pentahydroxybenzophenone, and mangostanaxanthone VI, respectively. To the best of our knowledge, this is the first report of the potential of xanthones and benzophenones to interact with *C. acnes* KAS III. Molecular dynamics simulations using GROMACS indicated that the JNK1-garcinoxanthone T complex had the highest stability of all ligand-protein complexes, with a high number of hydrogen bonds predicted to form between this ligand and its target. Petra/Osiris/Molinspiration (POM) analysis was also conducted to determine pharmacophore sites and predict the molecular properties of ligands influencing ADMET. All ligands, except for mangostanaxanthone VI, showed good membrane permeability. Garcinoxanthone T, gentisein and 2,4,6,3',5'-pentahydroxybenzophenone were identified as the most promising compounds to explore further, including in experimental studies, for their anti-acne potential.

Keywords: *Garcinia mangostana;* anti-acne; benzophenones; xanthones; molecular docking; molecular dynamics

1. Introduction

Acne vulgaris is one of the most common skin conditions experienced by teenagers and young adults [1]. It is characterised by the presence of comedones and inflammatory lesions (papules,

pustules and nodules) which occur when the pilosebaceous follicles become obstructed as a result of abnormal hyperkeratinisation, overproduction of sebum and proliferation of the acne-causing bacterium *Cutibacterium acnes* [2,3]. Mild to moderate acne is treated with topical drugs (i.e. retinoids, benzoyl peroxide, azelaic acid, antibiotics) with or without oral antibiotics. Severe cases of acne require hormonal treatment to reduce sebum production or the use of oral isotretinoin. These drugs, however, have adverse side effects ranging from mild skin irritation (most topical treatments) to teratogenicity (isotretinoin) that often lead to patients abandoning their treatment [4,5]. The rise in the emergence of antibiotic-resistant *C. acnes* strains is further cause for concern [6] and warrants the search for alternative anti-acne therapies.

There has been a growing interest over the past decade in the investigation of medicinal plants for the treatment of acne, with studies reporting the anti-acne potential of various plant extracts, often perceived to have less side-effects than conventional drugs [7-10]. In traditional south east Asian medicine, *Garcinia mangostana* (mangosteen) fruits have a history of use for inflammatory skin conditions, including acne [11-12]. Studies have previoulsy demonstrated the effectiveness of formulations containing mangosteen fruit extracts against acne inflammatory lesions, with antibacterial and anti-inflammatory effects attributed to xanthones such as α- and γ-mangostin [13-18]. Despite evidence to support the use of mangosteen in the treatment of acne, the precise mechanisms of action underlying its effect at the molecular level has been less well explored. To the best of our knowledge, there has been only one report on the anti-acne mode of action of *Garcinia mangostana* constituents [19]. As part of our research work using *in silico* approaches to investigate the therapeutic potential of natural products [20-27], we report herein on the anti-acne potential of *G. mangostana* xanthones and benzophenones using an *in silico* approach. Molecular docking and molecular dynamic (MD) simulations studies were performed to predict the interactions of *G. mangostana* xanthones and benzophenones with three proteins associated with acne pathogenesis. These were the human

c-Jun N-terminal kinase (JNK)1, a protein associated with the release of inflammatory mediators, along with KAS III and exo-β-1,4-mannosidase, two enzymes essential for the survival and proliferation of *C. acnes,* in the pilosebaceous unit [28-30].

2. Materials and Methods

2.1. Molecular docking

2.1.1. Preparation of proteins

The three-dimensional crystal structures of human JNK1 (PDB ID: 3V3V), *C. acnes* KAS III (PDB ID: 6A9N) and *C. acnes* exo-β-1,4-mannosidase (PDB ID: 6GVB) were retrieved from the RSCB Protein Data Bank (PDB) database (http://www.pdb.org). In preparation for the docking, all water molecules and heteroatoms were removed from the proteins using BIOVIA Discovery Studio Visualizer 2021. Polar hydrogen atoms were added using Autodock Tools v. 1.5.6. and the prepared proteins were saved in PDBQT format for docking.

2.1.2. Preparation of ligands

A total of 104 phytochemicals (97 xanthones and 7 benzophenones), unambiguously characterised and previously isolated from the pericarps (whole fruits) of *G. mangostana* L. (Clusiacaseae), were selected as the ligands for the molecular docking [12, 31-77]. Phloretin was used as the control inhibitory ligand for *C. acnes* KAS III [28]. All structures were drawn using ChemDraw v.20.1.1 and geometry-optimised using MM2 energy minimisation in this software. Gasteiger charges were added to each ligand and all rotatable bonds were made non-rotatable using Autodock Tools v. 1.5.6. All prepared ligands were saved in PDBQT format for docking.

2.1.3 Identification of binding sites and grid box preparation

The X, Y, Z coordinates of the JNK1 binding site were retrieved from the data stored within the crystallized protein structure [78]. The PrankWeb ligand binding site prediction online software (https://prankweb.cz/) was used to identify the most likely binding sites for *C. acnes* KAS III and *C. acnes* exo-β-1,4-mannosidase [79]. The X, Y, Z coordinates for the top-scoring binding pockets were subsequently used as the coordinates of the centre of the grid box. The size of each grid box was set at 22 × 22 × 22 points in each direction, with a spacing at 1 Å, ensuring that all phytochemicals could be accommodated within the binding site of each protein.

2.1.4. Molecular docking calculations

Autodock Vina v.1.5.6 was used to calculate the predicted free binding energy or docking scores (ΔG in kcal/mol) of each ligand against the selected protein targets. The default values set in Autodock Vina were used as the parameters for the docking (exhaustiveness = 8). Size-independent ligand efficiency (SILE) values were calculated to rank each ligand [80]. The ligands with the lowest free binding energy and highest SILE values were considered as the best binding ligands. The intermolecular interactions between the best ligands and the binding sites of the studied proteins were visualized in BIOVIA Discovery Studio 2021 Client. The contribution of hydrogen bonds to binding was evaluated in terms of bond lengths and Donor-H-Acceptor (DHA) angles [81].

2.2. Molecular dynamics (MD) simulations

The MD simulations were performed using the GROningen MAchine for Chemical Simulations (GROMACS) 4.6.7 package [82] with a CHARM27 all-atom force field. The topology files for the proteins were prepared using GROMACS, while the ligand topologies were obtained from the SwissParam server [83]. The system was neutralised by adding Na^+

and Cl^- ions, and the cubic TIP3P water model was used to solvate the complex system. The simulation process involved several steps, including minimisation, temperature equilibrium (NVT), pressure equilibrium (NPT) and was performed over a 20 ns time period at 310 °K with a time step of 2 fs to explore the dynamics of each protein interacting with the selected (best docked) ligands. Root means square deviations (RMSD), root means square fluctuations (RMSF), number of hydrogen bonds, radius of gyration (Rg), Coulombic short-range (Coul-SR), Lennard-Jones (LJ-SR) interaction energies and total non-bonded interaction energies computations were used to analyse the trajectories.

2.3. Petra/Osiris/Molinspiration (POM) analysis

The ligands selected for the MD simulation study were subjected to POM analysis to identify their pharmacophore site(s) – highlighting the electrostatic and steric effects that influence biological activity – and calculate the physicochemical parameters to predict ADMET profiles and drug-likeness using MarvinSketch v.23.4.0 (https://www.chemaxon.com), and the OSIRIS Property Explorer (https://www.organic-chemistry.org/prog/peo/) and Molinspiration servers (https://www.molinspiration.com/services/).

3. Results

3.1 Identification of the JNK1, *C. acnes* KAS III and *C. acnes* exo-β-1,4-mannosidase binding pockets

PrankWeb predictions revealed 6 and 17 likely binding site pockets for *C. acnes* KAS III and *C. acnes* exo-β-1,4-mannosidase, respectively. The top-scoring prediction was identified as the most probable binding site for each of these two enzymes (Figure S1, S2 and Table S1, S2). All grid box centre coordinates are presented in Table 1.

3.2. Molecular docking of ligands against JNK1, *C. acnes* KAS III and *C. acnes* exo-β-1,4-mannosidase

Garcinoxanthone T showed the best docking score (-11.5 kcal/mol) and the highest SILE value (4.4) against JNK1. In comparison, quercetagetin had a docking score of -11.0 kcal/mol and a SILE values of 4.3. Garcinoxanthone T showed several intermolecular interactions with amino acid residues of the JNK1 binding pocket. In particular, it formed hydrogen bonds with Ser34 (2.184 Å), Asp169 (2.283 Å), Met111 (1.648 Å), Glu109 (2.010 Å) including a strong interaction with Met111 (2.743 Å, DHA angle 162°). In addition, it formed several hydrophobic interactions with Val40, Ala53, Leu168, and Val158 (distances > 3.480 Å) (Figure 1 and Table 2, S3, S4).

The top-scoring binding pocket for *C. acnes* KAS III was predicted to contain a total of 29 amino acid residues (Table S1). Gentisein showed the best docking score (-8.9 kcal/mol) and highest SILE value (3.7) against *C. acnes* KAS III, and it was observed that one benzophenone, namely 2,4,6,3',5'-pentahydroxybenzophenone, also showed a high docking score (-8.6 kcal/mol) and SILE value (3.6). In comparison, the known inhibitor phloretin had a docking score of -7.8 kcal/mol and a SILE value of 3.2. Gentisein and 2,4,6,3',5'-pentahydroxybenzophenone displayed several intermolecular interactions with amino acid residues in the *C. acnes* KAS III binding pocket. Gentisein formed hydrogen bonds with Ser162 (2.985 Å) and Asn260 (3.034 Å). In addition, it formed an electrostatic H-bond type interaction with Arg262 (3.877 Å) and several hydrophobic interactions with Leu166, Arg223, Val225, and Ala259 (distances > 4.895 Å). On the other hand, 2,4,6,3',5'-pentahydroxybenzophenone formed hydrogen bonds with Asn260 (2.864, 2.846 Å) and Arg262 (2.210 Å). In addition, it formed an electrostatic H-bond with Arg223 (4.092 Å) and one hydrophobic interaction with Val225 (4.885 Å) (Figure 2, 3 and Table 2, S3, S4).

The top-scoring binding pocket for *C. acnes* exo-β-1,4-mannosidase was predicted to contain a total of 18 amino acid residues (Table S2). Mangostanaxanthone VI showed the best docking score (-13.2 kcal/mol) and the highest SILE value (4.5) against *C. acnes* exo-β-1,4-mannosidase. This compound formed several intermolecular interactions with the target enzyme. It showed hydrogen bonds with Gly150 (2.142 Å), Ser89 (2.877 Å) including a strong interaction with His86 (2.375 Å, DHA angle 162°). In addition, if formed electrostatic interactions with His151 (4.063 and 4.238 Å) as well as several hydrophobic interactions with Trp295, His151, Phe219, Trp217, Ala220, and Leu314 (distances > 3.660 Å) (Figure 4 and Table 2, S3, S4). Garcinoxanthone T, gentisein, 2,4,6,3',5'-pentahydroxybenzophenone and mangostanaxanthone VI were selected for further molecular dynamics simulations studies.

3.2. MD simulation studies

3.2.1. RMSD analysis

The average root mean square deviations (RMSD) values obtained for the C-alpha backbone protein atoms of each protein-ligand complex are presented in Figure 5 and Table 3. The lowest and highest RMSD values were obtained for JNK1-garcinoxanthone T (0.2093 ± 0.0194) and *C. acnes* exo-β-1,4-mannosidase-mangostanaxanthone VI (and 0.5909 ± 0.0339 nm), respectively.

3.2.2. RMSF analysis

The average root mean square fluctuation (RMSF) values of protein atoms identifying amino acid residues showing fluctuations in the presence of ligands are presented in Figure 6 and Table 3. Some JNK1 amino acid residues (Lys55, Glu73 and Asp169) exhibited low fluctuations while others (residues 1 to 10, 250 to 270 and 361 to 363) showed high RMSF values, but on average, the JNK1-garcinoxanthone T complex had the lowest RMSF value

(0.1016 ± 0.0345). The fluctuation patterns observed for the *C. acnes* KAS III-2,4,6,3',5' pentahydroxybenzophenone and *C. acnes* KAS III-gentisein complexes revealed that these two systems had similar protein flexibility throughout the MD simulation. A high RMSF value was obtained for the *C. acnes* exo-β-1,4-mannosidase-mangostanaxanthone VI complex.

3.2.3. Number of H-bonds analysis

Garcinoxanthone T and mangostanaxanthone VI formed the highest maximum number of hydrogen bonds (7) with JNK1 and *C. acnes* exo-β-1,4-mannosidase, respectively. The maximum number of hydrogen bonds formed by 2,4,6,3',5'pentahydroxybenzophenone and gentisein with *C. acnes* KAS III was fewer (5 and 2, respectively, with modes of 0) (Table 3). Garcinoxanthone T was predicted to form the highest number of hydrogen bonds with JNK1 over the entire MD simulation period (Figure 7).

3.2.4. Rg analysis

The *C. acnes* KAS III-ligand complexes had the lowest Rg values (1.9343 ± 0.0085 and 1.9178 ± 0.0076 for *C. acnes* KAS III-2,4,6,3',5' pentahydroxybenzophenone and *C. acnes* KAS III-gentisein, respectively). The *C. acnes* exo-β-1,4-mannosidase-mangostanaxanthone VI complex displayed the highest Rg value (3.028 ± 0.0122). The JNK1-garcinoxanthone T showed the highest degree of variation in Rg values (2.1843 ± 0.0171) (Table 3).

3.2.5. Calculations of interaction energies

The average interaction energy values computed for all protein-ligand complexes were < 0 kJ/mol. The *C. acnes* exo-β-1,4-mannosidase-mangostanaxanthone VI showed the highest total interaction energy value (-335.31 ± 21.18), followed by the JNK1-garcinoxanthone T complex

(-259.38 ± 22.21). The *C. acnes* KAS III-2,4,6,3',5'pentahydroxybenzophenone complex had the lowest interaction energy value (-103.5 ± 27.48 kJ/mol) (Figure 8 and Table 4).

3.3. POM analysis

3.3.1 Identification of pharmacophore sites

The predicted pharmacophore sites and charge localisation for the selected ligands are illustrated in Figure 9. The oxygen atoms of the carbonyl group and of the xanthone pyrone ring were negatively-charged (δ^-). The hydroxyl groups on all ligands were positively-charged (δ^+). Pharmacophore sites were identified as ($O^{\delta-}$----$OH^{\delta+}$) with the carbonyl oxygen intrachelated to a phenolic hydroxyl.

3.3.2 Osiris calculations

Toxicity risk predictions revealed that 2,4,6,3',5'-pentahydroxybenzophenone could be considered non-toxic overall, while garcinoxanthone T, gentisein, and mangostanaxanthone VI were likely to be associated with mutagenic risks only. Mangostanaxanthone VI and garcinoxanthone T showed the highest cLogP (octanol/water partition coefficient) values of 6.78 and 3.01, respectively. The solubility values (LogS) for all ligands ranged between -6.9 and -2.24. The ligands 2,4,6,3',5'pentahydroxy-benzophenone and mangostanaxanthone VI were estimated to be the most soluble and insoluble ligands, respectively. The molecular weights (MW) of the selected ligands ranged between 244 (gentisein) and 486 (mangostanaxanthone VI). All ligands had a negative drug-likeness (DL), with gentisein showing the best DL (-0.03). The overall drug scores (DS) (i.e. combining drug-likeness, cLogP, logS, MW and toxicity risk calculations) for the ligands ranged between 0.08 and 0.47 (Table 5).

249

250 3.3.3. Molinspiration calculations

251 The Molinspiration calculations are presented in Table 6. Mangostanaxanthone VI showed the
252 highest miLogP value of 7.53. All compounds displayed TPSA values < 140 $Å^2$, with
253 2,4,6,3',5'pentahydroxybenzophenone and gentisein having TPSA values < 120 $Å^2$. All
254 ligands, except for mangostanaxanthone VI, showed zero violation of the Lipiniski's 'rule-of-
255 five'. Mangostanaxanthone VI showed one violation of this rule. The molinspiration
256 calculations further showed that all ligands had the potential to interact with various enzymatic
257 targets as nuclear receptor ligand (NRL) and enzyme inhibitor (EI). Garcinoxanthone T was
258 further predicted to be a good potential G-protein coupled receptor (GPCR) ligand and kinase
259 inhibitor (KI). Mangostanaxanthone VI was predicted to be a potential GPCR ligand while
260 2,4,6,3',5' pentahydroxybenzophenone was predicted to be a possible ion channel modulator
261 (ICM) and KI candidate (Table 6).

262

263 **4. Discussion**

264 The release of pro-inflammatory mediators and the proliferation of acnegenic *C. acnes* in the
265 pilosebaceous units are two of the main factors involved in the pathogenesis of acne [84, 85].
266 *In vitro* studies using human keratinocytes have established that *C. acnes* triggers an
267 inflammatory response in the host via enhancing the phosphorylation of proteins involved in
268 the mitogen-activated protein kinase (MAPK) and nuclear transcription factor (NF-κB)
269 pathways, including c-Jun N-terminal kinases (JNK) such as JNK1 [19, 86]. Experimental
270 studies have previously demonstrated that selective JNK inhibitors exert anti-inflammatory
271 effects via reducing the production of pro-inflammatory cytokines [87, 88]. KAS III and exo-
272 β-1,4-mannosidase are two enzymes essential to the survival and proliferation of *C. acnes*.
273 KAS III (3-ketoacyl-ACP synthases) catalyse the condensation between acetyl-CoA and
274 malonyl ACP to form acetoacetyl-ACP in the initiation step of bacterial fatty acid biosynthesis.

The low homology of KAS III to other condensing enzymes in humans makes it an attractive target for the development of new antibacterial agents, including anti-acne medicines [28, 29, 89]. The exo-β-1,4-mannosidase enzyme enables *C. acnes* to hydrolyse the β-1,4 glycosidic bond between the second *N*-acetylglucosamine and the first mannose residue of eukaryotic *N*-glycans. This releases simple sugars that *C. acnes* uses as a nutrition source and also degrade immunoglobulin-linked *N*-glycans, which provides *C. acnes* with the ability to modulate the host's immune response to its advantage [30].

In our molecular docking study, garcinoxanthone T showed the highest predicted binding affinity and ligand efficiency for JNK1, greater than those of the known inhibitor quercetagetin. It also formed several interactions with amino acid residues of the JNK1 binding pocket, including some directly involved in the catalytic function of this enzyme in agreement with a previous report [78]. The top-scoring binding pocket for *C. acnes* KAS III contained Cys122, Val225, His257, Ala259, Asn260, previously reported as being involved in the catalytic function of this enzyme, as well as Ser162, Met220, Leu166, previously identified as binding residues for the phloretin control ligand [28]. Gentisein and 2,4,6,3',5'-pentahydroxybenzophenone both showed docking and ligand efficiency scores against *C. acnes* KAS III higher than those obtained for the known inhibitor phloretin. They interacted with Ser162, Leu166, Val225, Ala259, and Asn260 of *C. acnes* KAS III in agreement with a previous report [28]. The top-scoring binding pocket for *C. acnes* exo-β-1,4-mannosidase contained the catalytic residues Asn139, Glu140, Trp217, Glu259, and Trp295, as well as Ser88 and His151, previously identified as binding residues for the natural substrate of this enzyme [30]. Mangostanaxanthone VI showed the best docking and SILE score against *C. acnes* exo-β-1,4-mannosidase and interacted with His151 and Trp295 in agreement with a previous report [30].

The MD simulation was performed over 20 ns, as per recent studies that have evaluated the stability of other protein-ligand complexes over such a time period [90-92]. The RMSD of the C-alpha backbone protein atoms provided information on the stability of each system (with low values indicating high stability) while the RMSF values were used to identify fluctuations of individual amino acids (with low values indicating low fluctuations and high stability) [93-95]. The *C. acnes* exo-β-1,4-mannosidase-mangostanaxanthone VI complex was predicted to be the most unstable (highest RMSD value) of all complexes. All other complexes showed better stability trends. *C. acnes* KAS III showed good stability when bound to 2,4,6,3',5' pentahydroxybenzophenone, but was more unstable when bound to gentisein from 8 ns onwards. The JNK1-garcinoxanthone T complex displayed the most stable behaviour from 7 ns until the end of the MD simulation. It also showed on average less fluctuations compared to other complexes. This was particularly observed for Lys55, Glu73 and Asp169 which have been previously identified as amino acid residues directly involved in the catalytic activity of JNK1 [78].

Hydrogen bonding plays an important role in the stabilisation of ligands within the binding pocket of a given protein, with a high predicted number of hydrogen bonds indicating good stability of the resulting complex [96]. The highest number of hydrogen bonds formed between garcinoxanthone T and JNK1 was in line with the greater stability predicted for this complex in the RMSD and RMSF analyses. The radius of gyration (Rg) was further computed to evaluate the compactness of each protein bound to its ligands, with a low Rg value indicating good compactness [96]. The *C. acnes* KAS III-ligands and *C. acnes* exo-β-1,4-mannosidase-mangostanaxanthone VI complexes showed the highest and lowest compactness, respectively. Interestingly, the JNK1-garcinoxanthone T complex showed the highest degree of variation in compactness. The presence of low and high fluctuations obtained in RMSF analysis for certain amino acids of JNK1 upon binding to garcinoxanthone T may provide an explanation for this

finding. In particular, the interaction of garcinoxanthone T via a strong hydrogen bond to residues in the *N*-terminal lobe of JNK1 (e.g. Asp169) could potentially reorient this part of the protein in a similar way to what has been reported for the known inhibitor quercetagetin [78]. All interaction energy values of non-bonded interactions (i.e. electrostatic and van der Waals represented by the Coulombic and Lennard-Jones potential, respectively) between ligands and their protein targets had negative values, indicating favourable interactions [97, 98]. The high values obtained for the *C. acnes* exo-β-1,4-mannosidase-mangostanaxanthone VI and the JNK1-garcinoxanthone T complexes can be attributed to the specific characteristics of the pocket residues involved, namely Lys55, Asp169, Glu73, and Glu109 in JNK1 and Glu140, Glu259, His215, and Arg41 in *C. acnes* exo-β-1,4-mannosidase. These residues are charged, which enables them to engage in more electrostatic interactions. Additionally, the high lipophilicity and volume of mangostanaxanthone VI facilitate the formation of stronger van der Waals interactions compared to other ligands.

POM analysis was conducted to identify the pharmacophore sites and calculate the parameters predicting and ADMET profile of the selected ligands [99-102]. It is interesting to note that the pharmacophores identified are known to be associated with antibacterial activity [99, 103]. *Garcinia* xanthones/benzophenones containing this type of pharmacophore have demonstrated activity against Gram positive bacteria [49, 104-106]. This includes α- and γ-mangostin from *G. mangostana* which have previously shown potent activity against *C. acnes* [19, 107]. All ligands, except for mangostanaxanthone VI, showed zero violation of the Lipiniski's 'rule-of-five' and were also predicted to have good intestinal absorption potential (TPSA < 140 $Å^2$), indicating favourable oral bioavailability [108-111]. 2,4,6,3',5'pentahydroxybenzophenone and gentisein showed potential for oral activity through the transcellular route (TPSA < 120 $Å^2$) [112]. Gentisein was also found to have the lowest number of hydrogen bond

acceptor/donor atoms, predicting that this compound had the best skin permeability amongst all ligands [113].

Conclusion

Following molecular docking, molecular dynamics simulations and POM investigations, garcinoxanthone T, gentisein and 2,4,6,3',5'-pentahydroxybenzophenone were identified as the most promising ligands to explore further for their anti-acne potential. *In vitro* work has previously established that xanthones such as α- and γ-mangostin can suppress the *C. acnes*-induced expression of pro-inflammatory mediators, including TNF-α, IL-1β, and IL-6, in keratinocytes by inhibiting the activation of NF-κB and MAPK signalling pathways [19]. To the best of our knowledge, the present study is the first to report the ability of xanthones and benzophenones to interact with *C. acnes* KAS III. Further biological work is required to confirm these findings.

Acknowledgments: NB would like to thank the Oleg Polunin Memorial Trust and Modern Botany Ltd for contributing to her PhD scholarship.

Research ethics: Not applicable.

Author contributions: The authors have accepted responsibility for the entire content of this manuscript and approved its submission. NB and ZBA conducted the *in silico* study. VS and DR supervised the work. VS, NB and ZBA designed the study, analysed the results and prepared the manuscript. VS, NB, ZBA drafted the original manuscript. VS, DR, NB and SJ finalized the manuscript.

Competing Interests: The authors state no conflict of interest.

Research funding: None declared.

Data availability: The raw data can be obtained on request from the corresponding author.

References

[1] Layton, A. M., Thiboutot, D., & Tan, J. (2021). Reviewing the global burden of acne: how could we improve care to reduce the burden? *Journal of Dermatology*, *184*(2), 219-225.

[2] Cong, T. X., Hao, D., Wen, X., Li, X. H., He, G., & Jiang, X. (2019). From pathogenesis of acne vulgaris to anti-acne agents. *Archives of Dermatological Research*, *311*(5), 337-349.

[3] Dréno, B., Pécastaings, S., Corvec, S., Veraldi, S., Khammari, A. & Roques, C. (2018). *Cutibacterium acnes (Propionibacterium acnes)* and acne vulgaris: a brief look at the latest updates. *Journal of the European Academy of Dermatology and Venereology, 32,* 5-14.

[4] Habeshian, K. A., & Cohen, B. A. (2020). Current Issues in the Treatment of Acne Vulgaris. *Pediatrics*, *145* (Suppl 2), s225-s230.

[5] Sevimli Dikicier, B. (2019). Topical treatment of acne vulgaris: efficiency, side effects, and adherence rate. *Journal of International Medical Research*, *47(7),* 2987-2992. doi:10.1177/0300060519847367

[6] Karadag, A. S., Aslan Kayıran, M., Wu, C. Y., Chen, W., & Parish, L. C. (2021). Antibiotic resistance in acne: changes, consequences and concerns. *Journal of the European Academy of Dermatology and Venereology*, *35*(1), 73-78.

[7] Fisk, W. A, Lev-Tov, H. A., & Sivamani, R. K. (2014). Botanical and phytochemical therapy of acne: a systematic review. *Phytotherapy Research*, *28(8),* 1137-1152. doi:10.1002/ptr.5125

[8] Lambrechts, I. A., Canha, M. N., & Lall, N. (2018). Chapter 4. Exploiting Medicinal Plants as Possible Treatments for Acne Vulgaris.In: Medicinal Plants for Holistic Health and Well-Being, Lall N. (Ed). Academic Press, pp. 117-143.

[9] Nasri, H., Bahmani, M., Shahinfard, N., Moradi Nafchi, A., Saberianpour, S., & Rafieian Kopaei, M. (2015). Medicinal Plants for the Treatment of Acne Vulgaris: A Review of Recent Evidences. *Jundishapur Journal of Microbiology,* 8(11):e25580.

401 [10] Proença, A. C., Luís, Â., & Duarte, A. P. (2022). The Role of Herbal Medicine in the
402 Treatment of Acne Vulgaris: A Systematic Review of Clinical Trials. *Evidence Based*
403 *Complementary and Alternative Medicine, 2022,* 2011945. doi: 10.1155/2022/2011945.
404 [11] Maneenoon, K., Khuniad, C., Teanuan, Y., Saedan, N., Prom-In, S., Rukleng, N., ... &
405 Wongwiwat, W. (2015). Ethnomedicinal plants used by traditional healers in
406 Phatthalung Province, Peninsular Thailand. *Journal of Ethnobiology and*
407 *Ethnomedicine*, *11*(1), 1-20.
408 [12] Obolskiy, D., Pischel, I., Siriwatanametanon, N., & Heinrich M. (2009). *Garcinia*
409 *mangostana* L.: a phytochemical and pharmacological review. *Phytotherapy Research,*
410 *23*(8), 1047-1065.
411 [13] Khumsupan, P., & Gritsanapan, W. (2014). Anti-acne activity of *Garcinia mangostana*
412 L.: A review. *Plant Science Today, 1,* 147-150.
413 [14] Krisdaphong, T., & Jedsadapaisid, S. (2012). Antimicrobial activity of *Garcinia*
414 *mangostana* extract for anti-acne therapy. *International Federation of Societies of*
415 *Cosmetic Chemists (IFSCC) Magazine, 1,* 9-12.
416 [15] Lueangarun, S., Sriviriyakul, K., Tempark, T., Managit, C., & Sithisarn. P. (2019).
417 Clinical efficacy of 0.5% topical mangosteen extract in nanoparticle loaded gel in
418 treatment of mild-to-moderate acne vulgaris: A 12-week, split-face, double-blinded,
419 randomized, controlled trial. *Journal of Cosmetic Dermatology 18(*5), 1395-1403.
420 [16] Pan-In, P., Wongsomboon, A., Kokpol, C., Chaichanawongsaroj, N., &
421 Wanichwecharungruang, S. (2015). Depositing α-mangostin nanoparticles to sebaceous
422 gland area for acne treatment. *Journal of Pharmacological Sciences, 129*(4), 226-232.
423 [17] Pothitirat, W., Chomnawang, M. T., & Gritsanapan, W. (2010). Anti-acne-inducing
424 bacterial activity of mangosteen fruit rind extracts. *Medical Principles and*
425 *Practice*, *19*(4), 281-286.
426 [18] Sukatta, U., Rugthaworn, P., Pitpiangchan, P., & Dilokkunanant, U. (2008).
427 Development of mangosteen anti-acne gel. *Agriculture and Natural Resources*, *42*(5),
428 163-168.
429 [19] Xu, N., Deng, W., He, G., Gan, X., Gao, S., Chen, Y., ... & Hu, Z. (2018). Alpha-and
430 gamma-mangostins exhibit anti-acne activities via multiple
431 mechanisms. *Immunopharmacology and Immunotoxicology*, *40*(5), 415-422.
432 [20] Abdalla, M., Mohapatra, R. K., Sarangi, A.K., Mohapatra, P. K., Ali Eltayb, W., Alam,
433 M., …& Dhama, K. (2021). In silico studies on phytochemicals to combat the emerging

COVID-19 infection. *Journal of the Saudi Chemical Society*,*25*(12),101367. doi.org/10.1016/j.jscs.2021.101367

[21] Ali, M.T., Blicharska, N., Shilpi, J.A., & Seidel, V. (2018). Investigation of the anti-TB potential of selected propolis constituents using a molecular docking approach. *Scientific Reports, 8*(1):12238. doi: 10.1038/s41598-018-30209-y.

[22] Ben Ahmed, Z., Hefied, F., Mahammed, T. H., Seidel, V., & Yousfi, M. (2022). Identification of potential anti-Alzheimer agents from *Pistacia atlantica* Desf. galls using UPLC fingerprinting, chemometrics, and molecular docking analyses. *Journal of Food Processing and Preservation, 46(*10),e16916. doi: 10.1111/jfpp.16916

[23] Qasaymeh, R.M., Rotondo, D., Oosthuizen, C.B., Lall, N., & Seidel, V. (2019). Predictive Binding Affinity of Plant-Derived Natural Products Towards the Protein Kinase G Enzyme of *Mycobacterium tuberculosis* (*Mt*PknG). *Plants (Basel), 8*(11):477. doi: 10.3390/plants8110477.

[24] Shilpi, J.A., Ali, M.T., Saha, S., Hasan, S., Gray, A.I., & Seidel, V. (2015). Molecular docking studies on InhA, MabA and PanK enzymes from *Mycobacterium tuberculosis* of ellagic acid derivatives from *Ludwigia adscendens* and *Trewia nudiflora*. *In Silico Pharmacology, 3*(1), 10. doi: 10.1186/s40203-015-0014-1

[25] Shirlaw, O., Billah, Z., Attar, B., Hughes, L., Qasaymeh, R.M., Seidel, V., & Efthimiou G. (2020). Antibiofilm Activity of Heather and Manuka Honeys and Antivirulence Potential of Some of Their Constituents on the DsbA1 Enzyme of *Pseudomonas aeruginosa*. *Antibiotics (Basel), 9*(12):911. doi: 10.3390/antibiotics9120911.

[26] Siraj, M. A., Howlader, M. S. I., Rahaman, M. S., Shilpi, J. A., & Seidel, V. (2020). Antinociceptive and sedative activity of *Vernonia patula* and predictive interactions of its phenolic compounds with the cannabinoid type 1 receptor. *Phytotherapy Research, 35*(2),1069-1079. doi: 10.1002/ptr.6876.

[27] Siraj, M. A., Rahman, M. S., Tan, G. T., & Seidel, V. (2021). Molecular docking and molecular dynamics simulation studies of triterpenes from *Vernonia patula* with the cannabinoid type 1 receptor. *International Journal of Molecular Sciences*, *22*(7):3595. doi: 10.3390/ijms22073595.

[28] Cheon, D., Kim, J., Jeon, D., Shin, H.-C., & Kim, Y. (2019a). Target proteins of phloretin for its anti-inflammatory and antibacterial activities against *Propionibacterium acnes*-induced skin infection. *Molecules*, *24*(7), 1319.

[29] Cheon, D., Lee, W. C., Lee, Y., Lee, J. Y., & Kim, Y. (2019b). Structural basis of branched-chain fatty acid synthesis by *Propionibacterium acnes* β-ketoacyl acyl Carrier

protein synthase. *Biochemical and Biophysical Research Communications*, *509*(1), 322-328.

[30] Reichenbach, T., Kalyani, D., Gandini, R., Svartström, O., Aspeborg, H., & Divne, C. (2018). Structural and biochemical characterization of the *Cutibacterium acnes* exo-β-1, 4-mannosidase that targets the *N*-glycan core of host glycoproteins. *PloS One*, *13*(9), e0204703.

[31] Abdallah, H. M., El-Bassossy, H. M., Mohamed, G. A., El-Halawany, A. M., Alshali, K. Z., & Banjar, Z. M. (2017). Mangostanaxanthones III and IV: advanced glycation end-product inhibitors from the pericarp of *Garcinia mangostana*. *Journal of Natural Medicines*, *71*(1), 216-226.

[32] Al-Massarani, S. M., El Gamal, A. A., Al-Musayeib, N. M., Mothana, R. A., Basudan, O. A., Al-Rehaily, A. J., Farag, M., Assaf, M. H., El Tahir, K. H., & Maes, L. (2013). Phytochemical, antimicrobial and antiprotozoal evaluation of *Garcinia mangostana* pericarp and α-mangostin, its major xanthone derivative. *Molecules*, *18*(9), 10599-10608.

[33] Asai, F., Tosa, H., Tanaka, T., & Iinuma, M. (1995). A xanthone from pericarps of *Garcinia mangostana*. *Phytochemistry*, *39*(4), 943-944.

[34] Balasubramanian, K., & Rajagopalan, K. (1988). Novel xanthones from *Garcinia mangostana*, structures of BR-xanthone-A and BR-xanthone-B. *Phytochemistry*, *27*(5), 1552-1554.

[35] Chae, H. S., Kim, E. Y., Han, L., Kim, N. R., Lam, B., Paik, J. H., Yoon, K. D., Choi, Y. H., & Chin, Y. W. (2016). Xanthones with pancreatic lipase inhibitory activity from the pericarps of *Garcinia mangostana* L.(Guttiferae). *European Journal of Lipid Science and Technology*, *118*(9), 1416-1421.

[36] Chairungsrilerd, N., Takeuchi, K., Ohizumi, Y., Nozoe, S., & Ohta, T. (1996). Mangostanol, a prenyl xanthone from *Garcinia mangostana*. *Phytochemistry*, *43*(5), 1099-1102.

[37] Chin, Y.-W., Jung, H.-A., Chai, H., Keller, W. J., & Kinghorn, A. D. (2008). Xanthones with quinone reductase-inducing activity from the fruits of *Garcinia mangostana* (Mangosteen). *Phytochemistry*, *69*(3), 754-758.

[38] Du, C. T., & Francis, F. J. (1977). Anthocyanins of mangosteen, *Garcinia mangostana*. *Journal of Food Science*, *42*(6), 1667-1668.

[39] Fu, M., Qiu, S. X., Xu, Y., Wu, J., Chen, Y., Yu, Y., & Xiao, G. (2013). A new xanthone from the pericarp of *Garcinia mangostana*. *Natural Product Communications*, *8*(12), 1934578X1300801219.

[40] Gopalakrishnan, G., & Balaganesan, B. (2000). Two novel xanthones from *Garcinia mangostana*. *Fitoterapia*, *71*(5), 607-609.

[41] Gopalakrishnan, G., Banumathi, B., & Suresh, G. (1997). Evaluation of the antifungal activity of natural xanthones from Garcinia mangostana and their synthetic derivatives. *Journal of Natural Products*, *60*(5), 519-524.

[42] Huang, Y.-L., Chen, C.-C., Chen, Y.-J., Huang, R.-L., & Shieh, B.-J. (2001). Three xanthones and a benzophenone from *Garcinia mangostana*. *Journal of Natural Products*, *64*(7), 903-906.

[43] Ibrahim, S., Abdallah, H., El-Halawany, A., Radwan, M., Shehata, I., Al-Harshany, E., Zayed, M., & Mohamed, G. (2018). Garcixanthones B and C, new xanthones from the pericarps of *Garcinia mangostana* and their cytotoxic activity. *Phytochemistry Letters*, *25*, 12-16.

[44] Ibrahim, S., Abdallah, H., El-Halawany, A., Nafady, A., & Mohamed, G. (2019a). Mangostanaxanthone VIII, a new xanthone from *Garcinia mangostana* and its cytotoxic activity. *Natural Product Research*, *33*(2), 258-265.

[45] Ibrahim, S., Mohamed, G., Elfaky, M., Al Haidari, R., Zayed, M., El-Kholy, A., & Khedr, A. (2019b). Garcixanthone A, a new cytotoxic xanthone from the pericarps of *Garcinia mangostana*. *Journal of Asian Natural Products Research*, *21*(3), 291-297.

[46] Ibrahim, S., Mohamed, G., Khayat, M., Ahmed, S., & Abo-Haded, H. (2019c). Garcixanthone D, a New Xanthone, and Other Xanthone Derivatives From *Garcinia mangostana* Pericarps: Their α-Amylase Inhibitory Potential and Molecular Docking Studies. *Starch-Stärke*, *71*(7-8), 1800354.

[47] Ibrahim, S., Mohamed, G., Khayat, M., Ahmed, S., & Abo-Haded, H. (2019d). α-Amylase inhibition of xanthones from *Garcinia mangostana* pericarps and their possible use for the treatment of diabetes with molecular docking studies. *Journal of Food Biochemistry*, *43*(5), e12844.

[48] Ibrahim, S., Mohamed, G., Khayat, M., Ahmed, S., Abo-Haded, H., & Alshali, K. (2019e). Mangostanaxanthone VIIII, a new xanthone from *Garcinia mangostana* pericarps, alpha-amylase inhibitory activity, and molecular docking studies. *Brazilian Journal of Pharmacognosy*, *29*, 206-212.

[49] Iinuma, M., Tosa, H., Tanaka, T., Asai, F., Kobayashl, Y., Shimano, R., & Miyauchi, K.-I. (1996a). Antibacterial activity of xanthones from guttiferaeous plants against methicillin-resistant *Staphylococcus aureus*. *Journal of Pharmacy and Pharmacology*, *48*(8), 861-865.

[50] Jiang, H. Z., Quan, X. F., Tian, W. X., Hu, J. M., Wang, P. C., Huang, S. Z., Cheng, Z. Q., Liang, W. J., Zhou, J., & Ma, X. F. (2010). Fatty acid synthase inhibitors of phenolic constituents isolated from *Garcinia mangostana*. *Bioorganic & Medicinal Chemistry Letters*, *20*(20), 6045-6047.

[51] Jung, H.-A., Su, B.-N., Keller, W. J., Mehta, R. G., & Kinghorn, A. D. (2006). Antioxidant xanthones from the pericarp of *Garcinia mangostana* (Mangosteen). *Journal of Agricultural and Food Chemistry*, *54*(6), 2077-2082.

[52] Li, P., Yang, Z., Tang, B., Zhang, Q., Chen, Z., Zhang, J., Wei, J., Sun, L., & Yan, J. (2019). Identification of Xanthones from the Mangosteen Pericarp that Inhibit the Growth of *Ralstonia solanacearum*. *ACS omega*, *5*(1), 334-343.

[53] Liu, Q., Li, D., Wang, A., Dong, Z., Yin, S., Zhang, Q., Ye, Y., Li, L., & Lin, L. (2016). Nitric oxide inhibitory xanthones from the pericarps of *Garcinia mangostana*. *Phytochemistry*, *131*, 115-123.

[54] Mahabusarakam, W., Wiriyachitra, P., & Taylor, W. C. (1987). Chemical constituents of *Garcinia mangostana*. *Journal of Natural Products*, *50*(3), 474-478.

[55] Manogna Reddy D, JainMatsumoto, K., Akao, Y., Kobayashi, E., Ohguchi, K., Ito, T., Tanaka, T., Iinuma, M., & Nozawa, Y. (2003). Induction of apoptosis by xanthones from mangosteen in human leukemia cell lines. *Journal of Natural Products*, *66*(8), 1124-1127.

[56] Mohamed, G., Ibrahim, S., Shaaban, M., & Ross, S. (2014). Mangostanaxanthones I and II, new xanthones from the pericarp of *Garcinia mangostana*. *Fitoterapia*, *98*, 215-221.

[57] Mohamed, G., Al-Abd, A., El-Halawany, A., Abdallah, H., & Ibrahim, S. (2017). New xanthones and cytotoxic constituents from *Garcinia mangostana* fruit hulls against human hepatocellular, breast, and colorectal cancer cell lines. *Journal of Ethnopharmacology*, *198*, 302-312.

[58] Sen, A., Sarkar, K., Mazumder, P., Banerji, N., Uusvuori, R., & Hase, T. A (1980). A xanthone from *Garcinia mangostana*. *Phytochemistry*, *19*(10), 2223-2225.

[59] Sen, A., Sarkar, K., Mazumder, P., Banerji, N., Uusvuori, R., & Hase, T. (1982). The structures of garcinones A, B and C: Three new xanthones from *Garcinia mangostana*. *Phytochemistry*, *21*(7), 1747-1750.

[60] Suksamrarn, S., Komutiban, O., Ratananukul, P., Chimnoi, N., Lartpornmatulee, N., & Suksamrarn, A. (2006). Cytotoxic prenylated xanthones from the young fruit of Garcinia mangostana. *Chemical and Pharmaceutical Bulletin*, *54*(3), 301-305.

[61] Suksamrarn, S., Suwannapoch, N., Phakhodee, W., Thanuhiranlert, J., Ratananukul, P., Chimnoi, N., & Suksamrarn, A. (2003). Antimycobacterial activity of prenylated xanthones from the fruits of *Garcinia mangostana*. *Chemical and Pharmaceutical Bulletin*, *51*(7), 857-859.

[62] Suksamrarn, S., Suwannapoch, N., Ratananukul, P., Aroonlerk, N., & Suksamrarn, A. (2002). Xanthones from the Green Fruit Hulls of *Garcinia mangostana*. *Journal of Natural Products*, *65*(5), 761-763.

[63] Tran, T. H., Le Huyen, T., Tran, T. M., Nguyen, T. A., Pham, T. B., & Nguyen Tien, D. (2016). A new megastigmane sulphoglycoside and polyphenolic constituents from pericarps of *Garcinia mangostana*. *Natural Product Research*, *30*(14), 1598-1604.

[64] Tran, T. H., Le, H. T., Nguyen, H. M., Tran, T. H., Do Thi, T., Nguyen, X. C., & Ha, M. T. (2021). Garcinoxanthones SV, new xanthone derivatives from the pericarps of *Garcinia mangostana* together with their cytotoxic and antioxidant activities. *Fitoterapia*, *151*, 104880.

[65] Wang, S., Li, Q., Jing, M., Alba, E., Yang, X., Sabaté, R., Han, Y., Pi, R., Lan, W., & Yang, X. (2016). Natural xanthones from *Garcinia mangostana* with multifunctional activities for the therapy of Alzheimer's disease. *Neurochemical Research*, *41*(7), 1806-1817.

[66] Xu, T., Deng, Y., Zhao, S., & Shao, Z. (2016). A new xanthone from the pericarp of *Garcinia mangostana*. *Journal of Chemical Research*, *40*(1), 10-11.

[67] Xu, Z., Huang, L., Chen, X.-H., Zhu, X.-F., Qian, X.-J., Feng, G.-K., Lan, W.-J., & Li, H.-J. (2014). Cytotoxic prenylated xanthones from the pericarps of *Garcinia mangostana*. *Molecules*, *19*(2), 1820-1827.

[68] Yang, L., Zhang, D., Li, J.-B., Zhang, X., Zhou, N., Zhang, W.-Y., & Lu, H. (2022). Prenylated xanthones with α-glucosidase and α-amylase inhibitory effects from the pericarp of *Garcinia mangostana*. *Journal of Asian Natural Products Research*, *24*(7), 624-633.

598 [69] Yang, R., Li, P., Li, N., Zhang, Q., Bai, X., Wang, L., Xiao, Y., Sun, L., Yang, Q., &
599 Yan, J. (2017). Xanthones from the pericarp of *Garcinia mangostana*. *Molecules*,
600 *22*(5), 683.
601 [70] Yoshimura, M., Ninomiya, K., Tagashira, Y., Maejima, K., Yoshida, T., & Amakura,
602 Y. (2015). Polyphenolic constituents of the pericarp of mangosteen (*Garcinia*
603 *mangostana* L.). *Journal of Agricultural and Food Chemistry*, *63*(35), 7670-7674.
604 [71] Yu, L., Zhao, M., Yang, B., Zhao, Q., & Jiang, Y. (2007). Phenolics from hull of
605 *Garcinia mangostana* fruit and their antioxidant activities. *Food Chemistry*, *104*(1),
606 176-181.
607 [72] Zarena, A., & Sankar, K. U. (2012). Isolation and identification of pelargonidin 3-
608 glucoside in mangosteen pericarp. *Food Chemistry*, *130*(3), 665-670.
609 [73] Zhang, Y., Song, Z., Hao, J., Qiu, S., & Xu, Z. (2010). Two new prenylated xanthones
610 and a new prenylated tetrahydroxanthone from the pericarp of *Garcinia mangostana*.
611 *Fitoterapia*, *81*(6), 595-599.
612 [74] Zhao, Y., Liu, J.-P., Lu, D., Li, P.-Y., & Zhang, L.-X. (2010). A new antioxidant
613 xanthone from the pericarp of *Garcinia mangostana* Linn. *Natural Product Research*,
614 *24*(17), 1664-1670.
615 [75] Zhao, Y., Liu, J.-P., Lu, D., Li, P.-Y., & Zhang, L.-X. (2012). Two new xanthones from
616 the pericarp of *Garcinia mangostana*. *Natural Product Research*, *26*(1), 61-65.
617 [76] Zhou, X., He, L., Wu, X., Zhong, Y., Zhang, J., Wang, Y., Wang, B., Xu, Z., & Qiu, S.
618 (2015). Two new xanthones from the pericarp of *Garcinia mangostana*. *Natural*
619 *Product Research*, *29*(1), 19-23.
620 [77] Zhou, X., Huang, R., Hao, J., Huang, H., Fu, M., Xu, Z., Zhou, Y., Li, X. E., Qiu, S. X.,
621 & Wang, B. (2011). Two new prenylated xanthones from the pericarp of *Garcinia*
622 *mangostana* (Mangosteen). *Helvetica Chimica Acta, 94*(11), 2092-2098.
623 [78] Baek, S., Kang, N. J., Popowicz, G. M., Arciniega, M., Jung, S. K., Byun, S., & Lee, K.
624 W. (2013). Structural and functional analysis of the natural JNK1 inhibitor
625 quercetagetin. *Journal of Molecular Biology*, *425*(2), 411-423.
626 [79] Jendele, L., Krivak, R., Skoda, P., Novotny, M., & Hoksza, D. (2019). PrankWeb: a
627 web server for ligand binding site prediction and visualization. *Nucleic Acids Research*,
628 *47*(W1), W345-W349.
629 [80] Nissink, J. W. M. (2009). Simple size-independent measure of ligand efficiency.
630 *Journal of Chemical Information and Modelling*, *49*(6), 1617-1622.

631 [81] Ferreira de Freitas, R., Schapira, M. (2017). A systematic analysis of atomic protein-
632 ligand interactions in the PDB. *Medicinal Chemistry Communications, 8*(10), 1970-
633 1981.
634 [82] Lemkul, J. A. (2018). From proteins to perturbed hamiltonians: A suite of tutorials for
635 the GROMACS-2018 molecular simulation package [article v1. 0]. *Living Journal of*
636 *Computational Molecular Science*, *1*(5068.10), 33011.
637 [83] Zoete, V., Cuendet, M. A., Grosdidier, A., & Michielin, O. (2011). SwissParam: a fast
638 force field generation tool for small organic molecules. *Journal of Computational*
639 *Chemistry, 32*(11), 2359-2368.
640 [84] Platsidaki, E., & Dessinioti, C. (2018). Recent advances in
641 understanding *Propionibacterium acnes* (*Cutibacterium acnes*) in acne.
642 *F1000Research, 7*, F1000 Faculty Rev-1953. doi: 10.12688/f1000research.15659.1.
643 [85] Tanghetti, E.A. (2013). The role of inflammation in the pathology of acne. *Journal of*
644 *Clinical and Aesthetic Dermatology, 6*(9):27-35.
645 [86] Li, W. H., Zhang, L., Lyte, P., Rodriguez, K., Cavender, D., & Southall, M. D. (2015).
646 p38 MAP Kinase Inhibition Reduces *Propionibacterium acnes*-Induced Inflammation
647 in Vitro. *Dermatology and Therapy (Heidelb*), 5(1):53-66.
648 [87] Graczyk, P.P. (2013). JNK inhibitors as anti-inflammatory and neuroprotective
649 agents. *Future Medicinal Chemistry, 5*(5), 539-551.
650 [88] Seledtsov, V.I., Malashchenko, V.V., Meniailo, M.E., Atochin, D.N., Seledtsova, G.V.,
651 Schepetkin, I.A. (2020). Inhibitory effect of IQ-1S, a selective c-Jun N-terminal kinase
652 (JNK) inhibitor, on phenotypical and cytokine-producing characteristics in human
653 macrophages and T-cells. *European Journal of Pharmacology, 878,* 173116.
654 [89] Nofiani, R., Philmus, B., Nindita, Y., & Mahmud, T. (2019). 3-Ketoacyl-ACP synthase
655 (KAS) III homologues and their roles in natural product biosynthesis. *Medicinal*
656 *Chemistry Communications,* 10,1517-1530.
657 [90] Adem, Ş., Eyupoglu, V., Sarfraz, I., Rasul, A., Zahoor, A. F., Ali, M., Abdalla M.,
658 Ibrahim I. M. & Elfiky, A. A. (2021). Caffeic acid derivatives (CAFDs) as inhibitors of
659 SARS-CoV-2: CAFDs-based functional foods as a potential alternative approach to
660 combat COVID-19. *Phytomedicine*, 85, 153310.
661 [91] Fatriansyah, J. F., Boanerges, A. G., Kurnianto, S. R., Pradana, A. F., Fadilah & Surip,
662 S. N. (2022). Molecular Dynamics Simulation of Ligands from *Anredera cordifolia*
663 (Binahong) to the Main Protease (M^{pro}) of SARS-CoV-2. *Journal of Tropical*
664 *Medicine*, 2022, 1178228.

[92] Kushwaha, P. P., Singh, A. K., Bansal, T., Yadav, A., Prajapati, K. S., Shuaib, M., & Kumar, S. (2021). Identification of natural inhibitors against SARS-CoV-2 drugable targets using molecular docking, molecular dynamics simulation, and MM-PBSA approach. Frontiers in Cellular and Infection Microbiology, 11, 730288.

[93] Badieyan, S., Bevan, D. R., & Zhang, C. (2012). Study and design of stability in GH5 cellulases. *Biotechnology and Bioengineering, 109*(1), 31-44.

[94] Martínez L. (2015). Automatic identification of mobile and rigid substructures in molecular dynamics simulations and fractional structural fluctuation analysis. *PLoS One, 10*(3):e0119264. doi: 10.1371/journal.pone.0119264.

[95] Purmonen M, Valjakka J, Takkinen K, et al. Molecular dynamics studies on the thermostability of family II xylanases. *Protein Engineering Design and Selection.* 20(11), 551-559(2007).

[96] Ahamad, S., Gupta, D., & Kumar, V. (2022). Targeting SARS-CoV-2 nucleocapsid oligomerization: Insights from molecular docking and molecular dynamics simulations. Journal of Biomolecular Structure and Dynamics, 40(6):2430-2443. doi: 10.1080/07391102.2020.1839563.

[97] Vijayabaskar, M. S., & Vishveshwara, S. (2010). Interaction energy based protein structure networks. *Biophysical Journal, 99*(11), 3704-15. doi: 10.1016/j.bpj.2010.08.079.

[98] Waidyasooriya, H. M., Hariyama, M., & Kasahara, K. (2017). An FPGA accelerator for molecular dynamics simulation using OpenCL. *International Journal of Networked and Distributed Computing, 5*(1), 52-61. doi: 10.2991/ijndc.2017.5.1.6

[99] Hadda, T. B., Fergoug, T., Warad, I., Masand, V., & Sheikh, J. (2013). POM as a quick bioinformatic platform to select flavonoids and their metabolites as potential and efficient HIV-1 integrase inhibitors. *Research on Chemical Intermediates*, *39*, 1227-1244.

[100] Hadda, T. B., Rastija, V., AlMalki, F., et al. (2021). Petra/Osiris/Molinspiration and Molecular Docking Analyses of 3-Hydroxy-Indolin-2-one Derivatives as Potential Antiviral Agents. *Current Computer-Aided Drug* Design, 17(1):123-133. doi:10.2174/1573409916666191226110029

[101] Jarrahpour, A., Fathi, J., Mimouni, M., Hadda, B. T., Sheikh J., Chohan, Z., & Parvez, A. (2012). Petra, Osiris and Molinspiration (POM) together as a successful support in drug design: antibacterial activity and biopharmaceutical characterization of some azo

698 Schiff bases. *Medicinal* Chemistry *Research, 21,* 1984-1990. doi.org/10.1007/s00044-
699 011-9723-0
700 [102] Tariq, M., Sirajuddin, M., Ali, S., Khalid, N., Tahir, M. N., Khan, H., Ansari, T. M.
701 (2016). Pharmacological investigations and Petra/Osiris/Molinspiration (POM)
702 analyses of newly synthesized potentially bioactive organotin(IV) carboxylates. *Journal*
703 *of Photochemistry and Photobiology B. Biology, 158,* 174-183.
704 doi:10.1016/j.jphotobiol.2016.02.028
705 [103] Abdelhady, M. I. S., Kamal, A. M., & Barghash, M.F. (2018). POM analyses,
706 immunomodulatory, cytotoxic activities and polyphenolic constituents of *Callistemon*
707 *viridiflorus* fruits, *Bulletin of Faculty of Pharmacy, Cairo University,56* (2), 175-178.
708 doi.org/10.1016/j.bfopcu.2018.06.001.
709 [104] Auranwiwat, C., Trisuwan, K., Saiai, A., Pyne, S. G., & Ritthiwigrom, T. (2014).
710 Antibacterial tetraoxygenated xanthones from the immature fruits of *Garcinia*
711 *cowa*. *Fitoterapia*, *98*, 179-183.
712 [105] Iinuma, M., Tosa, H., Tanaka, T., Kanamaru, S., Asai, F., Kobayashi, Y., Miyauchi, K.,
713 & Shimano, R. (1996b). Antibacterial activity of some *Garcinia* benzophenone
714 derivatives against methicillin-resistant *Staphylococcus aureus*. *Biological and*
715 *Pharmaceutical Bulletin, 19*(2),311-314. doi:10.1248/bpb.19.311.
716 [106] Koh, J. J., Qiu, S., Zou, H., Lakshminarayanan, R., Li, J., Zhou, X., ... & Beuerman, R.
717 W. (2013). Rapid bactericidal action of alpha-mangostin against MRSA as an outcome
718 of membrane targeting. *Biochimica et Biophysica Acta (BBA)-Biomembranes*, *1828*(2),
719 834-844.
720 [107] Asasutjarit, R., Meesomboon, T., Adulheem, P., Kittiwisut, S., Sookdee, P.,
721 Samosornsuk, W., & Fuongfuchat, A. (2019). Physicochemical properties of alpha-
722 mangostin loaded nanoemulsions prepared by ultrasonication technique. *Heliyon*, *5*(9),
723 e02465.
724 [108] Lipinski, C. A. (2000). Drug-like Properties and the Causes of Poor Solubility and Poor
725 Permeability. *Journal of Pharmacological and Toxicological Methods*, *44*, 235-249.
726 [109] Lipinski, C. A., Lombardo, F., Dominy, B. W., & Feeney, P. J. (2001). Experimental
727 and Computational Approaches to Estimate Solubility and Permeability in Drug
728 Discovery and Development Settings. *Advance Drug Delivery Reviews, 46*, 3-26.
729 [110] Palm, K., Luthman, K., Unge, A.-L., Strandlund, G., & Artursson, P. (1996).
730 Correlation of Drug Absorption with Molecular Surface Properties. *Journal of*
731 *Pharmaceutical Sciences, 85*, 32-39.

[111] Palm, K., Stenberg, P., Luthman, K., & Artursson, P. (1997). Polar Molecular Surface Properties Predict the Intestinal Absorption of Drugs in Humans. *Pharmaceutical Research*, *14*, 568-571.

[112] Van de Waterbeemd, H. In Silico Models to Predict Oral Absorption. In: Comprehensive Medicinal Chemistry II, Volume 5-ADME-Tox approaches, Chapter 5.28. Taylor JB and Triggle DJ Eds. Elsevier (Oxford) 2007, pp. 669–697.

[113] Kostal J (2016). Computational Chemistry in Predictive Toxicology: status quo et quo vadis? In: Advances in Molecular Toxicology, Fishbein JC, Heilman JM (Eds), Volume 10, pp. 139-186. Elsevier, Amsterdam, The Netherlands.

Table 1. Grid box centre X, Y, Z coordinates used for each target protein

Protein (PDB ID)	**X, Y, Z coordinates**
JNK1 (3V3V)	31.213, 44.393, 4.154
C. acnes KAS III (6A9N)	-8.6105, 22.3827, 173.0191
C. acnes Exo-β-1,4 mannosidase (6GVB)	20.7606, 8.3728, -67.607

760

761

762

763

764

765

766 **Table 2:** Molecular interactions of *G. mangostana* xanthones and benzophenones showing
767 the best docking scores and SILE values towards JNK1, *C. acnes* KAS III and *C. acnes* exo-
768 β-1,4-mannosidase.

Target protein	Ligand	Docking score (kcal/mol)	SILE	Interacting residues	Distance (Å)	Category	Type
JNK1	Garcino-xanthone T	-11.5	4.4	Ser34	2.184	H-Bond	Conventional
				Met111	1.648 2.743	H-Bond H-Bond	Conventional Conventional
				Asp169	2.283	H-Bond	Conventional
				Glu109	2.010	H-Bond	Conventional
				Val40	3.480 4.255	Hydrophobic Hydrophobic	Pi-Sigma Pi-Alkyl
				Leu168	3.844 4.934	Hydrophobic Hydrophobic	Pi-Sigma Pi-Alkyl
				Ala53	4.412 5.226	Hydrophobic Hydrophobic	Pi-Alkyl Pi-Alkyl
				Val158	4.941	Hydrophobic	Pi-Alkyl
***C. acnes* KAS III**	Gentisein	-8.9	3.7	Ser162	2.985	H-Bond	Conventional
				Arg262	3.877	Pi-Cation Pi-Donor, H-bond	Electrostatic H-Bond
				Asn260	3.034	H-bond	Pi-Donor H-Bond
				Leu166	5.272	Hydrophobic	Pi-Alkyl
				Val225	4.914	Hydrophobic	Pi-Alkyl
				Ala259	4.895	Hydrophobic	Pi-Alkyl
				Arg223	4.962	Hydrophobic	Pi-Alkyl
				Arg46		Unfavourable	
	2,4,6,3',5' Pentahydroxybenzo-phenone	-8.6	3.6	Asn260	2.864 2.846	H-Bond H-Bond	Conventional Pi-donor H-bond
				Arg 262	2.210	H-bond	Conventional
				Arg 223	4.092	H-bond; electrostatic	Pi cation, Pi donor, H-bond
				Val225	4.885	Hydrophobic	Pi-Alkyl
***C. acnes* Exo-β-1,4-manno-sidase**	Mangostana xanthone VI	-13.2	4.5	His86	2.375	H-bond	Conventional
				Ser89	2.877	H-bond	Conventional
				Gly150	2.142	H-bond	Conventional
				His 151	4.063 4.238	Electrostatic Electrostatic	Pi-Cation Pi-Cation
				Trp295	3.660 3.875 4.417 4.370	Hydrophobic Hydrophobic Hydrophobic Hydrophobic	Pi-Sigma Pi-Sigma Pi-Alkyl Pi-Alkyl
				His151	4.123 4.747	Hydrophobic Hydrophobic	Pi-Pi Stacked Pi-Pi Stacked
				Phe219	5.797 5.883	Hydrophobic Hydrophobic	Pi-Pi T-shaped Pi-Pi T-shaped
				Trp217	5.234 4.794 4.207	Hydrophobic Hydrophobic Hydrophobic	Pi-Alkyl Pi-Alkyl Pi-Alkyl
				Ala220	4.974	Hydrophobic	Pi-Alkyl
				Leu314	5.443	Hydrophobic	Alkyl

769

Table 3: Average values of RMSD, RMSF, Rg and number of hydrogen bonds for JNK1-garcinoxanthone T, *C. acnes* KAS III-2,4,6,3',5'pentahydroxybenzophenone, *C. acnes* KAS III-gentisein, and *C. acnes* exo-β-1,4-mannosidase-mangostanaxanthone VI complexes over the MD simulation period.

	JNK1-garcinoxanthone T	*C. acnes* KAS III-2,4,6,3',5' pentahydroxy-benzophenone	*C. acnes* KAS III-gentisein	*C. acnes* Exo-β-1,4-mannosidase-mangostanaxanthone VI
RMSD (nm)	0.2093 ± 0.0194	0.2696 ± 0.0231	0.2787 ± 0.0427	0.5909 ± 0.0339
RMSF (nm)	0.1016 ± 0.0345	0.1131 ± 0.0453	0.1027 ± 0.0437	0.1530 ± 0.0417
Maximum number of H-bonds (mode)	7 (5)	5 (0)	2 (0)	7 (3)
Rg	2.1843 ± 0.0171	1.9343 ± 0.0085	1.9178 ± 0.0076	3.028 ± 0.0122

Table 4: Average Coulombic short-range (Coul-SR), Lennard-Jones short-range (LJ-SR), and total interaction energy values for the JNK1-garcinoxanthone T, *C. acnes* KAS III-2,4,6,3',5'pentahydroxy-benzophenone, *C. acnes* KAS III-gentisein and *C. acnes* exo-β-1,4-mannosidase-mangostanaxanthone VI complexes over the MD simulation period.

Energy values (kJ/mol)	JNK1-garcinoxanthone T	*C. acnes* KAS III-2,4,6,3',5' pentahydroxy-benzophenone	*C. acnes* KAS III-gentisein	*C. acnes* Exo-β-1,4-mannosidase-mangostanaxanthone VI
Coul-SR	-134.433 ± 22.373	-29.522 ± 18.066	-12.8853 ± 5.693	-146.304 ± 19.96
LJ-SR	-124.947 ± 10.888	-73.9771 ± 15.71	-129.325 ± 6.587	-189.006 ± 13.058
Total	-259.38 ± 22.21	-103.5 ± 27.48	-142.21 ± 8.75	-335.31 ± 21.18

785 **Table 5:** Toxicity risks and ADMET parameters for the studied ligands, predicted using Osiris Property Explorer

Ligand	**MW (g/mol)**	**Toxicity risks**				**Osiris calculations**			
		MUT	**TUMO**	**IRRI**	**EoR**	**cLogP**	**Solubility (LogS)**	**DL**	**DS**
Garcinoxanthone T	346	🔴	🟢	🟢	🟢	3.01	-4.5	-1.86	0.24
Gentisein	244	🔴	🟢	🟢	🟢	2.33	-4.04	-0.03	0.36
2,4,6,3',5'pentahydroxy-benzophenone	262	🟢	🟢	🟢	🟢	1.06	-2.24	-5.62	0.47
Mangostanaxanthone VI	486	🔴	🟢	🟢	🟢	6.78	-6.9	-2.25	0.08

786 MUT: mutagenic, TUMO tumorigenic, IRRI: irritant (eyes and skin), EoR: effects on reproduction,
787 TPSA: total polar surface area, DL drug-likeness, DS drug-score 🟢 Low risk 🔴 High risk)

Table 6: Molinspiration calculations for the studied ligands

Ligand	miLogP	TPSA	nON / nOHNH	NV	VOL	GPCRL	ICM	KI	NRL	PI	EI
Garcinoxanthone T	2.81	131.35	7 / 5	0	295.9	0.1	-0.09	0.05	0.68	-0.06	0.43
Gentisein	2.27	90.89	5 / 3	0	196.63	-0.28	-0.20	-0.09	0.17	-0.49	0.23
2,4,6,3',5'pentahydroxy-benzophenone	1.72	118.21	6 / 5	0	214.53	0	0.02	0.17	0.24	-0.27	0.19
Mangostanaxanthone VI	7.53	131.35	7 / 5	1	463	0.08	-0.17	-0.14	0.56	-0.04	0.35

TPSA: Topological polar surface area; nON: Number of H-bond acceptor; nOHNH: Number of H-bond donor;
NV: number of violation of the Lipinski's rule of 5; VOL: volume; GPCRL: G-protein coupled receptor ligand;
ICM: Ion channel modulator; KI: Kinase inhibitor; NRL: Nuclear receptor ligand; PI: Protease inhibitor; EI: Enzyme inhibitor.

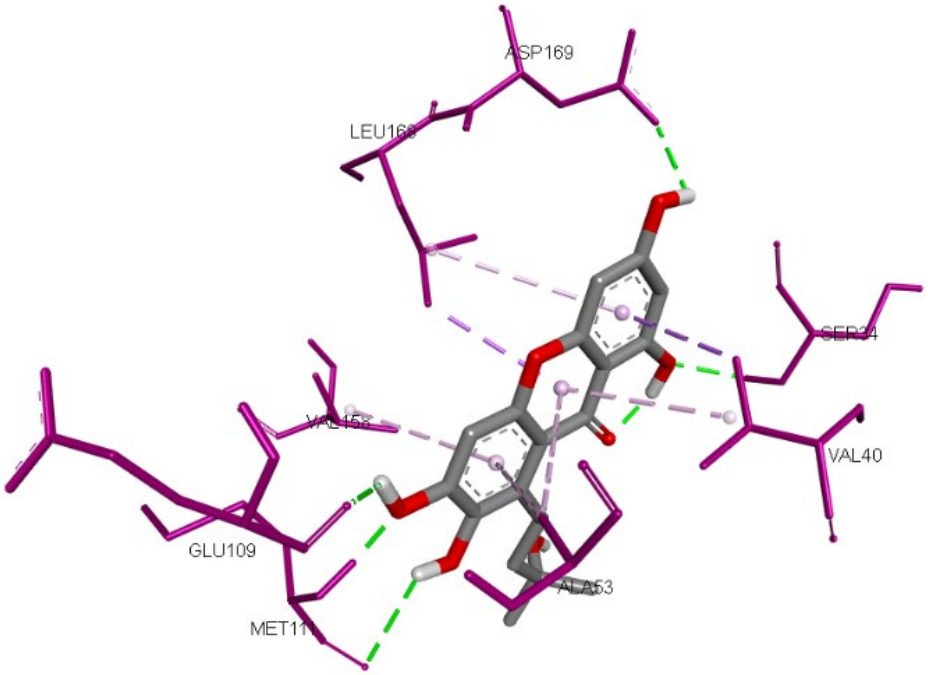

(a)

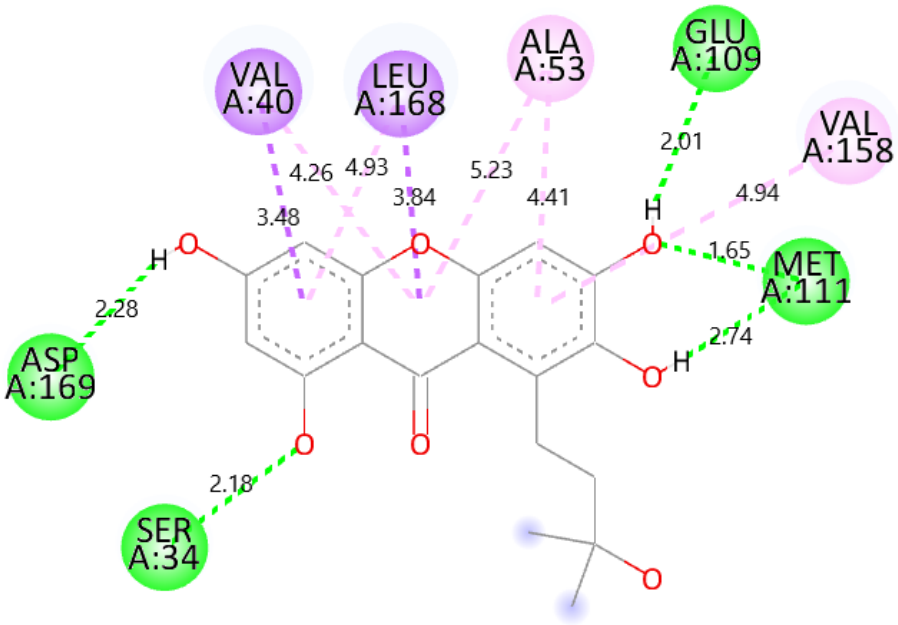

(b)

Figure 1: Predicted intermolecular interactions between garcinoxanthone T and JNK1. **(a)** Docked pose of garcinoxanthone T within the JNK1 binding pocket. **(b)** 2D representation of intermolecular interactions between garcinoxanthone T and respective amino acid residues of JNK1, showing conventional hydrogen (green) and hydrophobic (pink) bondings. Bond distances in angstroms.

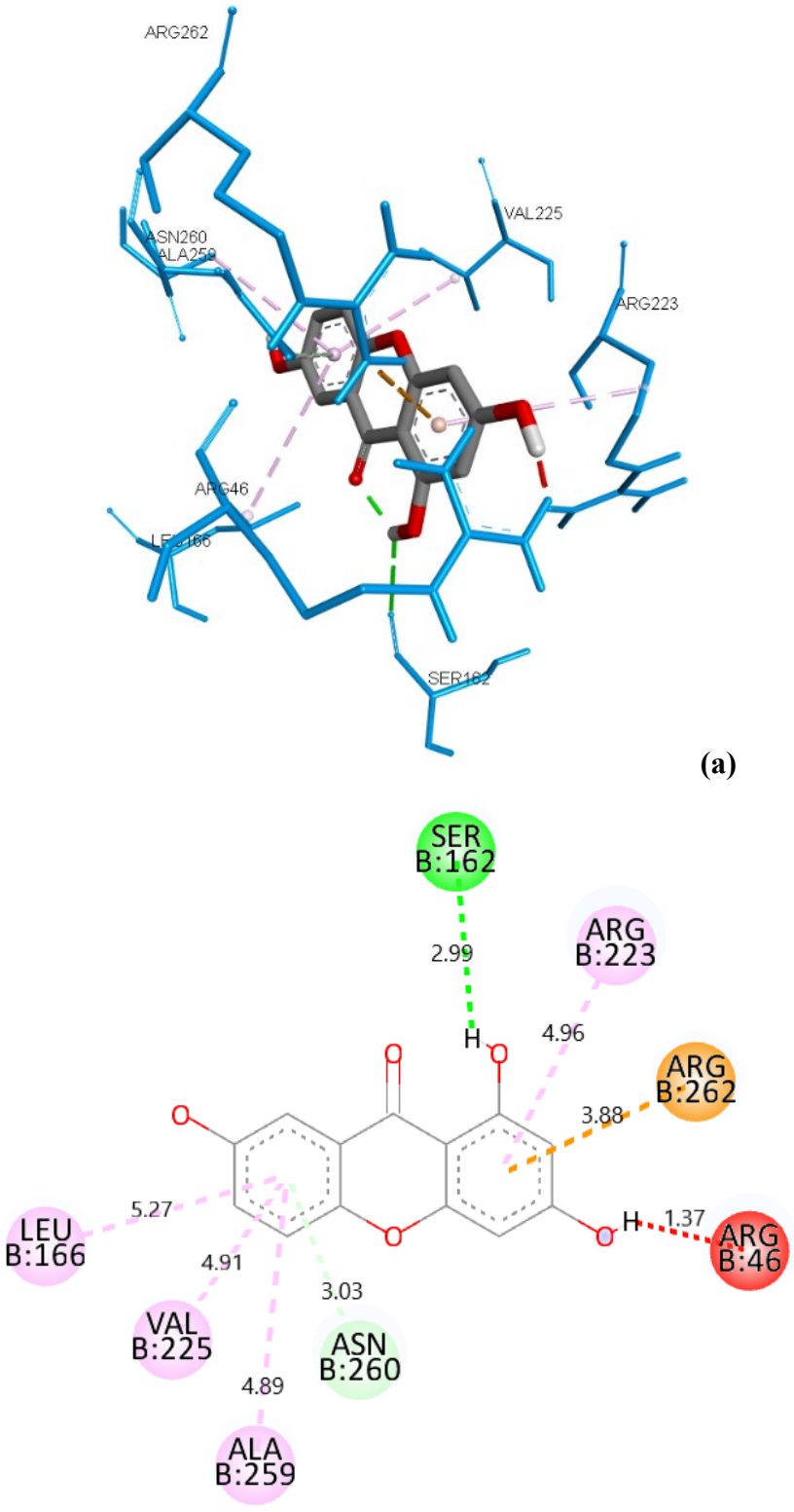

Figure 2: Predicted intermolecular interactions between gentisein and *C. acnes* KAS III. **(a)** Docked pose of gentisein within the *C. acnes* KAS III binding pocket. **(b)** 2D representation of intermolecular interactions between gentisein and respective amino acid residues of *C. acnes* KAS III, showing conventional hydrogen (dark green), Pi-donor hydrogen (pale green), electrostatic hydrogen (orange), hydrophobic (pink) and unfavourable (red) bondings. Bond distances in angstroms.

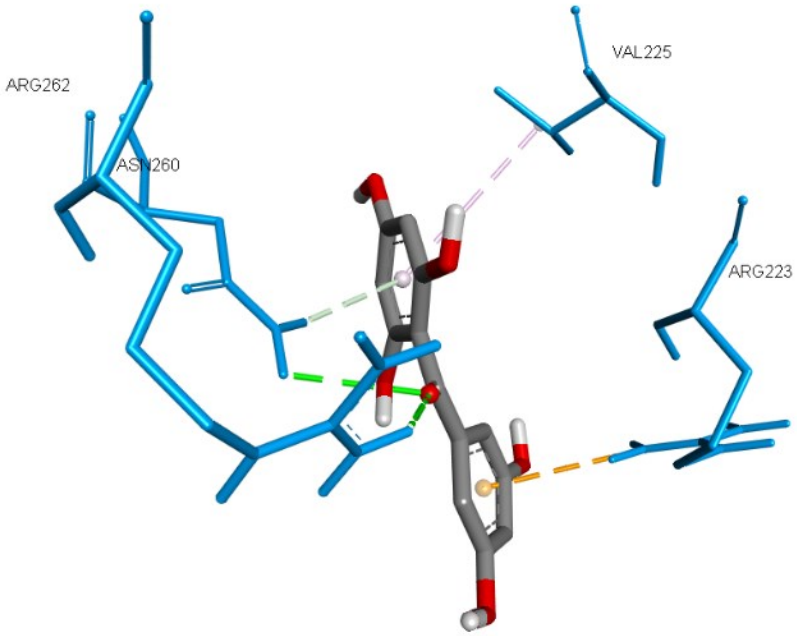

(a)

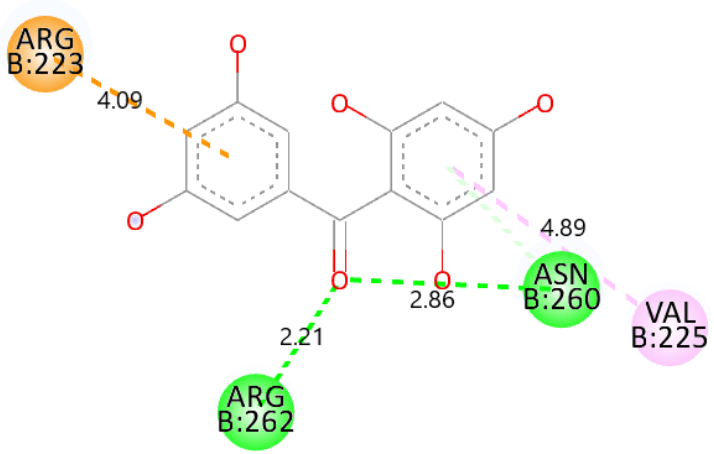

(b)

Figure 3: Predicted intermolecular interactions between 2,4,6,3',5'-pentahydroxy-benzophenone and *C. acnes* KAS III. **(a)** Docked pose of 2,4,6,3',5'-pentahydroxy-benzophenone within the *C. acnes* KAS III binding pocket. **(b)** 2D representation of intermolecular interactions between 2,4,6,3',5'-pentahydroxybenzophenone and respective amino acid residues of *C. acnes* KAS III, showing conventional hydrogen (dark green), Pi-donor hydrogen (pale green), electrostatic hydrogen (orange) and hydrophobic (pink) bondings. Bond distances in angstroms.

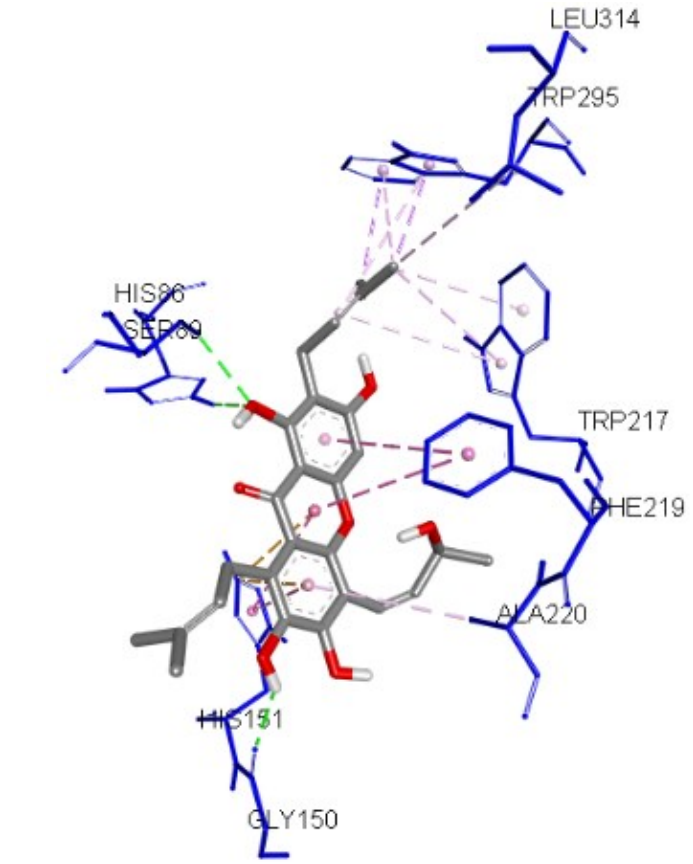

(a)

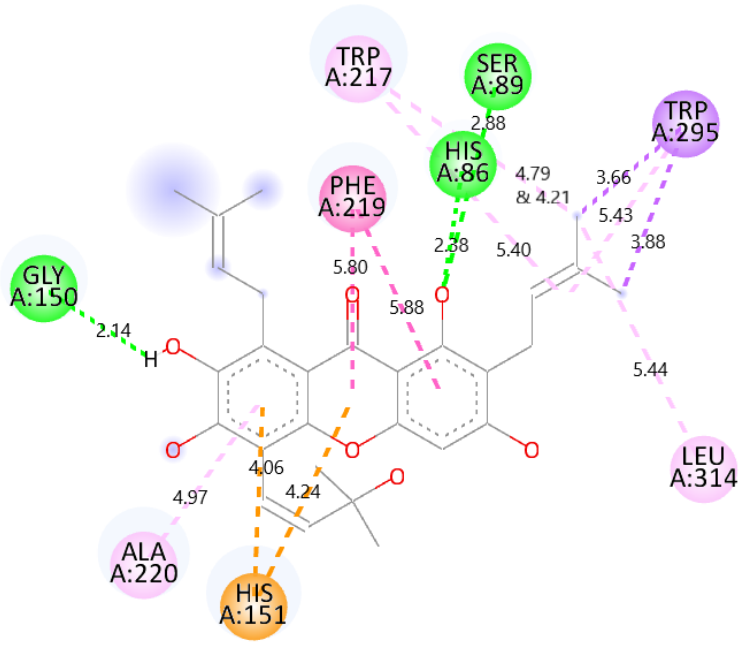

(b)

Figure 4: Predicted intermolecular interactions between mangostanaxanthone and *C. acnes* exo-β-1,4-mannosidase. **(a)** Docked pose of mangostanaxanthone within the *C. acnes* exo-β-1,4-mannosidase binding pocket. **(b)** 2D representation of intermolecular interactions between mangostanaxanthone and respective amino acid residues of *C. acnes* exo-β-1,4-mannosidase,

showing conventional hydrogen (green), electrostatic hydrogen (orange) and hydrophobic (pink) bondings. Bond distances in angstroms.

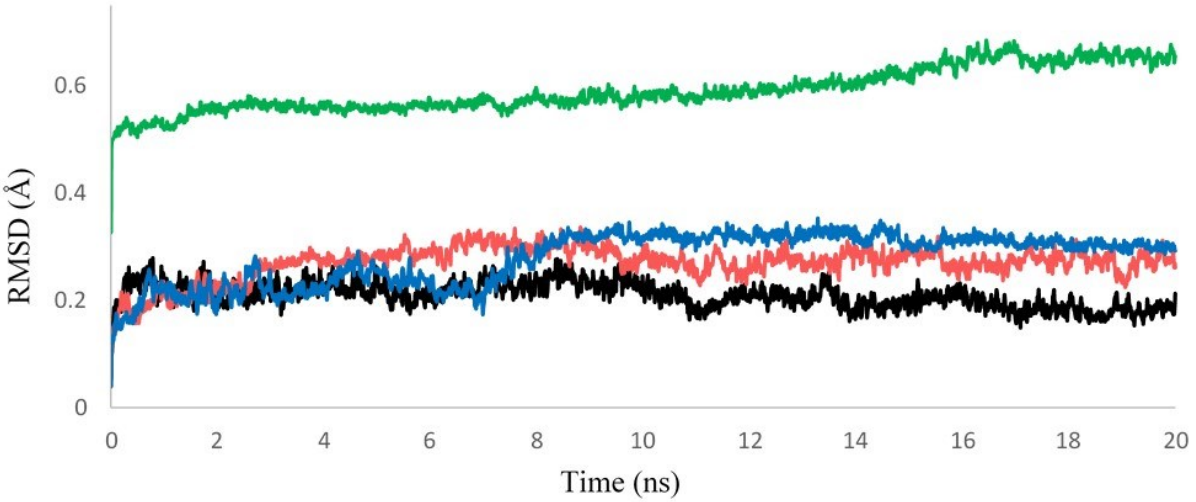

Figure 5: RMSD plots of JNK1-garcinoxanthone T (black), *C. acnes* KAS III-gentisein (blue), *C. acnes* KAS III-2,4,6,3',5'pentahydroxybenzophenone (red), and *C. acnes* exo-β-1,4-mannosidase-mangostana-xanthone VI (green) over the MD simulation period.

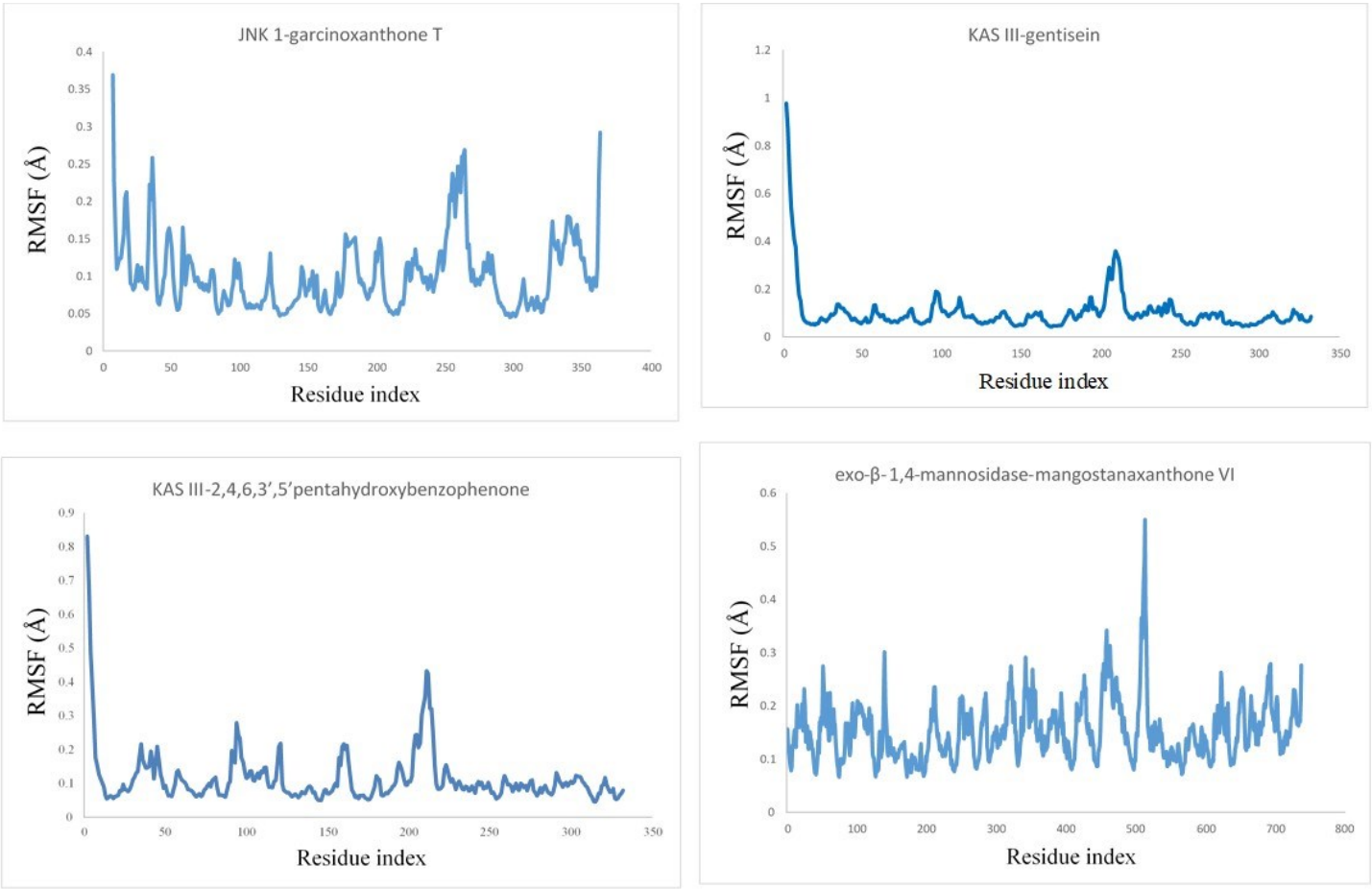

Figure 6: RMSF plots of JNK1-garcinoxanthone T, *C. acnes* KAS III-gentisein, *C. acnes* KAS III-2,4,6,3',5'penta-hydroxybenzophenone and *C. acnes* exo-β-1,4-mannosidase-mangostanaxanthone VI over the MD simulation period.

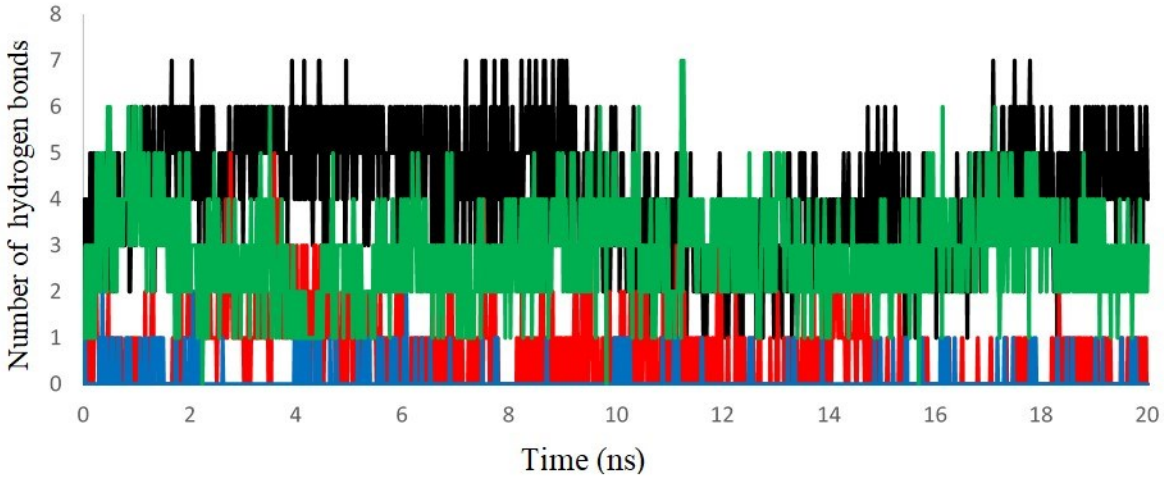

Figure 7: Assessment of the number of H-bonds formed between each protein-ligand complex over the MD simulation period. JNK1-garcinoxanthone T (black), *C. acnes* KAS III-gentisein (blue), *C. acnes* KAS III-2,4,6,3',5'penta-hydroxybenzophenone (red) and *C. acnes* exo-β-1,4-mannosidase-mangostana-xanthone VI (green).

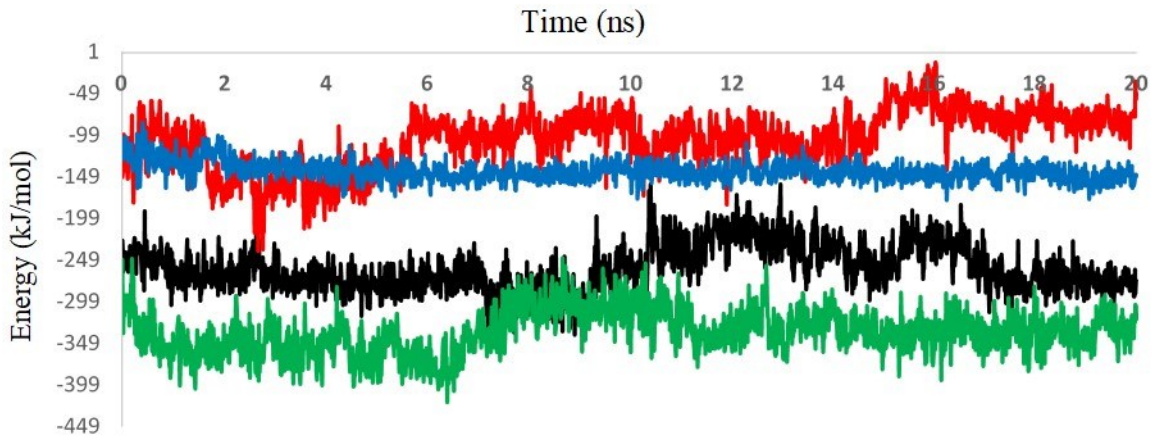

Figure 8: Total interaction energies plots of JNK1-garcinoxanthone T (black), *C. acnes* KAS III-gentisein (blue), *C. acnes* KAS III-2,4,6,3',5'penta-hydroxybenzophenone (red) and *C. acnes* exo-β-1,4-mannosidase-mangostanaxanthone VI (green) over the MD simulation period.

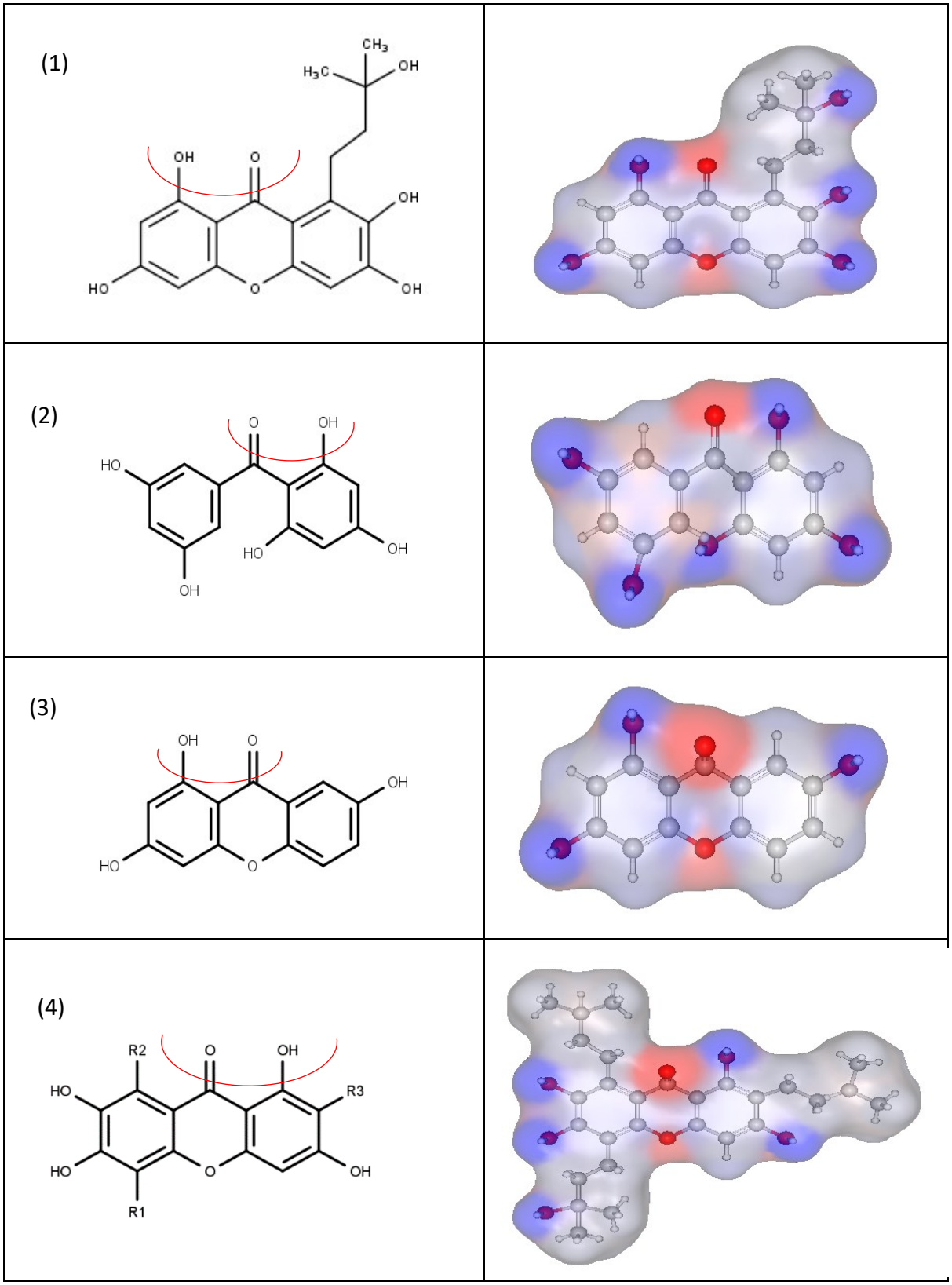

912 **Figure 9**: Predicted pharmacophore sites (within the red semi-circles) and charge localisation
913 for garcinoxanthone T (1), 2,4,6,3',5'penta-hydroxybenzophenone (2), gentisein (3) and
914 mangostanaxanthone VI (4). Positively-charged (δ^+) and negatively-charged (δ^-) centres in blue
915 and red, respectively.
916

917